Twenty-Seventh Symposium (International) on Combustion/The Combustion Institute, 1998/pp. 177–184

# MEASUREMENT OF THE RATE CONSTANT FOR H + $O_2$ + M → $HO_2$ + M (M = $N_2$, Ar) USING KINETIC MODELING OF THE HIGH-PRESSURE $H_2/O_2/NO_x$ REACTION

MARK A. MUELLER, RICHARD A. YETTER, AND FREDERICK L. DRYER
*Department of Mechanical and Aerospace Engineering*
*Princeton University*
*Princeton, NJ 08544, USA*

The reaction of dilute $H_2/O_2/N_2$ and $H_2/O_2$/Ar mixtures perturbed with small quantities of NO has been studied in a variable-pressure flow reactor between 800 and 900 K. At high pressures (10–14 atm), the consumption of $H_2$ and the conversion of NO to $NO_2$ were highly sensitive to the pressure-dependent reaction

$$H + O_2(+M) \xrightarrow{k_2} HO_2(+M)$$

Rate coefficient data for the low-pressure limit

$$H + O_2 + M \xrightarrow{k_{2,0}} HO_2 + M$$

were inferred by comparison of the experimental data with a reaction mechanism that uses the high-pressure limit $k_{2,\infty} = 4.52 \times 10^{13}\ (T/300)^{0.6}$ with $F_c^{N_2} = 0.5$ and $F_c^{Ar} = 0.45$. The data obtained with M = Ar are consistent with previous shock-tube data at comparable temperatures and are in good agreement with recent recommendations for $k_{2,0}^{Ar}$. However, the data obtained for M = $N_2$ are 40% lower than recent recommendations and are combined with previously published data to yield

$$k_{2,0}^{N_2} = 3.5 \times 10^{16}\ T^{-0.41}\ \exp(+1116/RT)\ \text{cm}^6\ \text{mole}^{-2}\ \text{s}^{-1}$$

over the temperature range 300–1600 K. The rate coefficient data obtained in this study are insensitive to the competing reaction

$$H + O_2 \xrightarrow{k_1} OH + O$$

and, when used with the $k_1$ recommendation from Pirraglia et al. [27], are in good agreement with $H_2/O_2$ explosion limit data in the intermediate temperature range of 700–900 K.

## Introduction

The termolecular reaction

$$H + O_2\ (+M) = HO_2\ (+M) \qquad (R2)$$

profoundly influences the kinetics of many reacting systems of practical importance. At low temperatures, reaction (2) efficiently converts H atoms to $HO_2$ radicals, thereby contributing to the $HO_x$ cycle of atmospheric chemistry [1]. At intermediate temperatures, the competition between reaction (2) and the branching reaction

$$H + O_2 = OH + O \qquad (R1)$$

for H atoms determines the explosion limit behavior [2] and ignition characteristics [3] of hydrogen–oxygen mixtures at conditions where $HO_2$ formation is terminating. With increasing pressure, the consumption of $HO_2$ via gas-phase reactions becomes increasingly important and can result in a shift in the explosion limit behavior of $H_2/O_2$ mixtures [2,4].

The extensive efforts to measure the low-pressure limit $k_{2,0}$ have been summarized in the reviews of Baulch et al. [5,6]. The high-pressure limit $k_{2,\infty}$ has been investigated by Cobos et al. [7], and the pressure-dependent rate constant $k_{2,\text{eff}}$ can be determined using the Troe formulation [8]. The determination of $k_{2,0}$ at temperatures of interest for combustion chemistry is complicated by competition between reactions 1 and 2, and, as a result, nearly all previous estimates of $k_{2,0}$ at temperatures in excess of 750 K have been quite sensitive to an assumed value for $k_1$. At conditions where $k_{2,\text{eff}} \gg k_1$, the kinetics of the unperturbed $H_2/O_2$ system are influenced by $HO_2$–$H_2O_2$ chemistry characterized by complex temperature dependencies indicative of

the formation of activated complexes [9,10]. However, as shown by Ashmore and Tyler [11], the addition of small quantities of $NO_x$ can greatly simplify the kinetic behavior of the system by providing an alternate consumption route for $HO_2$ radicals via

$$NO + HO_2 = NO_2 + OH \qquad (R3)$$

$NO_2$ can then react with H atoms via

$$NO_2 + H = NO + OH \qquad (R4)$$

to give back NO and thereby form a catalytic cycle that consumes $H_2$ at temperatures well below the explosion limits of the unperturbed system. At low $NO_x$ concentrations, essentially all the NO is oxidized to $NO_2$; however, increasing the $NO_x$ concentration beyond a threshold value leads to a $NO_2$ concentration that enables reaction 4 to compete effectively with reaction 2 for H atoms. In this case, a steady-state analysis of the $NO_2$ and $HO_2$ concentrations gives

$$[NO_2]_{SS} = \frac{k_{2,\text{eff}}[O_2]}{k_4} \qquad (1)$$

Bromly et al. [12] recently used this characteristic feature of the $H_2/O_2/NO_x$ system as part of a kinetic analysis of flow reactor data to estimate $k_2$ at atmospheric pressure over the temperature range 700–825 K.

This study extends the work of Bromly et al. [12] by investigating the $H_2/O_2/NO_x$ system over a range of pressures (10–14 atm) and temperatures (800–900 K) where $k_{2,\text{eff}} \gg k_1$. At these conditions, the flux of H atoms through the branching reaction is very small in comparison to reactions 2 and 4. Therefore, both the consumption of $H_2$ and the $NO/NO_2$ ratio are highly dependent upon $k_2$ and $k_4$ while being insensitive to $k_1$. Because the rate constant for reaction 4 is considered to be well characterized [13,14], the measurement of $H_2$ and $NO_x$ profiles of the perturbed high-pressure $H_2/O_2$ reaction offers a means to estimate $k_{2,0}$ with very little influence from the assumed value for $k_1$ at temperatures that overlap and extend beyond those studied by Bromly et al. Furthermore, the use of both $N_2$ and Ar as carrier gases permits the direct determination of the relative third-body efficiencies of these inert gases.

## Flow Reactor Experiment

The experimental apparatus used in this study is a variable-pressure (0.2–20 atm) turbulent flow reactor capable of operating to temperatures approaching 1200 K. The design and operating characteristics of this reactor have been discussed in detail elsewhere [15,16]. Nitrogen or argon carrier gas is heated by an electric resistance heater and mixed with oxygen as it enters a 10.2-cm-diameter quartz duct that serves as the test section. The remaining reactants ($H_2$ and NO) are diluted with inert gas and individually injected into the carrier gas at the entrance of a silica foam diffuser. The reacting mixture is sampled at axial locations downstream of the diffuser using a hot-water-cooled, stainless steel sampling probe that continuously extracts and convectively quenches a small percentage of the flow. The sample gas flows via heated Teflon lines to a series of analytical equipment that measure $H_2O$ ($\pm 10\%$), $NO_x$ ($\pm 5\%$), $O_2$ ($\pm 2\%$), and $H_2$ ($\pm 5\%$). The temperature of the reacting mixture is measured at the sampling location using a silica-coated type R thermocouple accurate to approximately $\pm 3$ K [15]. Test-section wall temperatures are controlled at the initial gas temperature to minimize heat loss from the reaction zone.

A computer-controlled stepper motor positions the injector and diffuser assembly with respect to the fixed sampling probe and enables residence times ranging from 1.5 ms to 3 s. In the vicinity of the injection point, mixing and diffusive effects are nonnegligible and influence the chemical induction time. However, the high convective velocities in the downstream test section suppress spatial gradients and permit the neglect of the diffusive terms in the governing equations. The test section can therefore be modeled as a zero-dimensional system using SENKIN [17] with isobaric and adiabatic assumptions provided there is no memory effect of the chemical perturbations in the mixing region. In an earlier paper [18], we have shown that for the $CO/H_2O/O_2$ system, such perturbations affect only the chemical induction times and not the reaction gradients in the test section. Similar analyses of the $H_2/O_2/NO_x$ reaction at the conditions of the present work have confirmed the same results. To facilitate comparison between the experimental data and model predictions, the data have been shifted in time to agree with model predictions at the point of 50% fuel consumption unless otherwise noted.

To determine $k_{2,0}$, we modeled our species profile measurements using our baseline $CO/H_2O/O_2/NO_x$ reaction mechanism [19] in which $k_{2,0}$ was treated as an adjustable parameter. The use of dilute mixtures ensures that the temperature rise in our experiments is rather modest (typically 70 K), and we simply assumed $k_{2,0}$ to be constant rather than impose a temperature dependency. Previous studies [20,21] have shown $k_{2,0}$ to be mildly temperature dependent, and errors attributable to this approximation are small in comparison to other experimental uncertainties. Least-squares analyses of the $H_2$, NO, and $NO_2$ profiles were used to obtain values of $k_{2,0}$ that resulted in the best agreement between experimental data and model predictions. The high-pressure limit of reaction 2 used in this study ($k_{2,\infty} = 4.52 \times 10^{13}\ (T/300)^{0.6}$ cm$^3$ mole$^{-1}$ s$^{-1}$ with $F_c^{N_2} = 0.5$ and $F_c^{Ar} = 0.45$) is slightly different than that

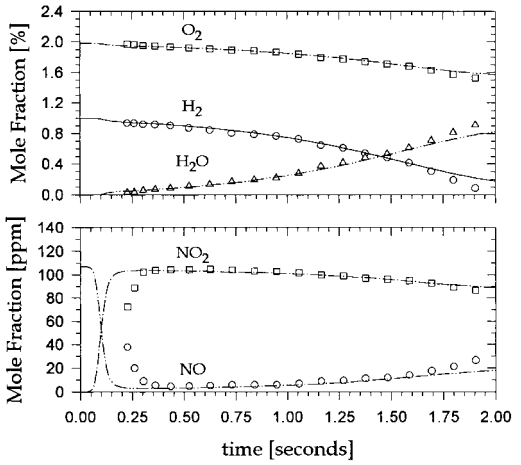


FIG. 1. Reaction profiles for a 1% $H_2$/2.0% $O_2$/107 ppm NO/$N_2$ mixture at $p$ = 12.5 atm and $T_i$ = 808 K. Symbols represent data points; lines represent predictions of baseline reaction mechanism with $k_{2,0}^{N_2}$ = 4.03 × $10^{15}$ $cm^6$ $mole^{-2}$ $s^{-1}$. Experimental data are shifted +0.138 s.

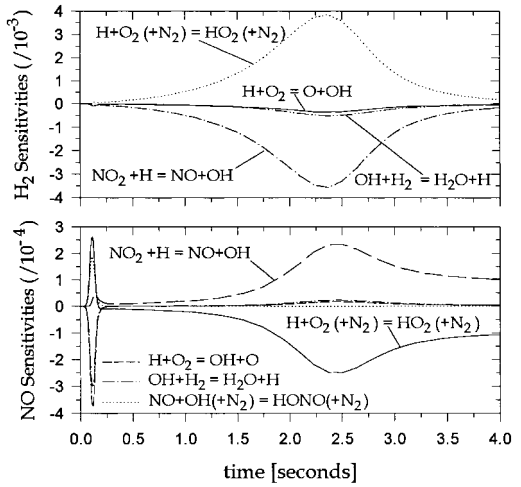


FIG. 2. Sensitivity coefficients ($S_{ij} = \partial Y_i/\partial \ln k_j$) for the $H_2$ and NO profiles shown in Fig. 1. $NO_2$ sensitivities are similar to those for NO but are of opposite sign.

used in our baseline mechanism ($k_{2,\infty}$ = 4.52 × $10^{13}$ $cm^3$ $mole^{-1}$ $s^{-1}$ with $F_c$ = 1.0). This new expression permits direct comparisons with the recent modeling efforts of Davidson et al. [22] and facilitates interpretation of data consistent with the recommendations of Cobos et al. [7].

## Experimental Results

Mixtures of 1% $H_2$/1–2% $O_2$/$N_2$ and 0.6% $H_2$/1.2% $O_2$/Ar perturbed with 30–110 ppm of NO were used to obtain the reaction profile measurements from which we determined $k_{2,0}$. An example of the experimental data obtained with M = $N_2$ is shown in Fig. 1 along with model predictions generated using an optimized value of $k_{2,0}^{N_2}$ = 4.03 × $10^{15}$ $cm^6$ $mole^{-2}$ $s^{-1}$. Results from gradient sensitivity analyses of this experiment are given in Fig. 2 and indicate that $H_2$ consumption is predominantly sensitive to $k_2$ and $k_4$ throughout the entire reaction. The NO mole fraction is likewise sensitive to $k_2$ and $k_4$ during the majority of the reaction; however, the rapid oxidation of NO to $NO_2$ that occurs early in the reaction is also sensitive to several other rate constants including that of H + $O_2$ = OH + O. As a result, the $NO_x$ data during this initial part of the reaction were not used in the least-squares analysis. This causes little difficulty in our efforts to determine $k_{2,0}^{N_2}$ because the kinetics that govern the $NO_x$ profiles during the remaining portion of the reaction are essentially decoupled from those that bring about the rapid conversion of NO to $NO_2$.

The disparity between the experimental and predicted NO and $NO_2$ profiles at early reaction times can be reduced by adjusting the rate constants for H + $O_2$ = OH + O, OH + $H_2$ = $H_2O$ + H, and NO + OH (+M) = HONO(+M) within their respective uncertainties. Such adjustments do not significantly (+7 to −2%) influence the determination of $k_{2,0}$. However, as a substantial percentage of the NO is oxidized to $NO_2$ in the mixing region prior to the first sampling location, we do not believe that comparisons between the model and $NO_x$ profile data during the initial portion of the reaction support modifications to the model. Moreover, the adjustment of these rate constants is inconsistent with experimental data for the $H_2$/$O_2$/$NO_x$ reaction at low pressures and for the unperturbed $H_2$/$O_2$ reaction over a wide range of conditions. By using higher convective velocities, the rapid oxidation of NO to $NO_2$ can be moved out of the mixing region and studied in more detail. However, this was not considered as part of the present study.

An example of the experimental data obtained using argon as the third body for reaction 2 is shown in Fig. 3. Due to the lower collision efficiency of argon relative to nitrogen, the flux of H atoms through reaction 4 increases proportionally and results in lower steady-state $NO_2$ concentrations than when M = $N_2$. The model predictions included in Fig. 3 were generated using $k_{2,0}^{Ar}$ = 2.33 × $10^{15}$ $cm^6$ $mole^{-2}$ $s^{-1}$. Results from gradient sensitivity analyses for this experiment are similar to those given in Fig. 2.

The experimental data obtained in this study are summarized in Table 1 in which we report $k_{2,0}$ values derived from the $H_2$, NO, and $NO_2$ profiles measured in each experiment. We also give an estimate of $k_{2,0}$ based upon the steady-state approximation given in equation 1, which is valid if reactions 2, 3,

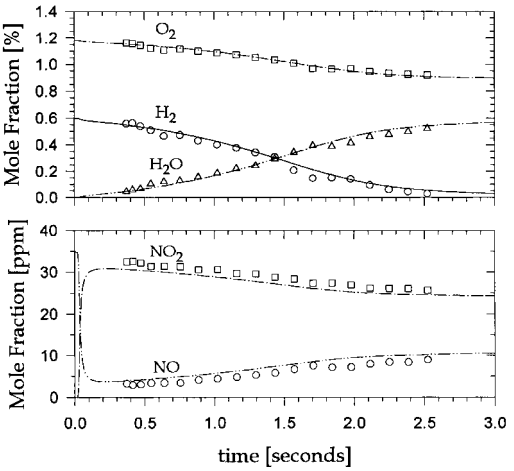


FIG. 3. Reaction profiles for a 0.6% $H_2$/1.2% $O_2$/35 ppm NO/Ar mixture at $p = 10$ atm and $T_i = 800$ K. Symbols represent experimental data; lines represent predictions of baseline model with $k_{2,0}^{Ar} = 2.33 \times 10^{15}$ cm$^6$ mole$^{-2}$ s$^{-1}$. Experimental data are shifted +0.258 s.

and 4 are the only important formation and consumption routes for $HO_2$ and $NO_2$. We note that the agreement among the values of $k_{2,0}$ obtained using the various profile measurements and the steady-state approximation is very good. Our data indicate that at temperatures near 850 K, the collision efficiency of nitrogen is 1.6 times greater than that of argon. This is in good agreement with previous estimates obtained at temperatures exceeding 1000 K [22–24] and somewhat lower than room-temperature measurements that vary from 2.2 to 3.4 [7,20,21,25,26].

We estimate that our determination of $k_{2,0}^{N_2}$ is accurate to within +30 to −23%. An uncertainty analysis, provided in Table 2, shows that the primary sources of uncertainty are associated with the recommended value of $k_4$ as well as the broadening factor used to estimate the falloff behavior of reaction 2. The uncertainty of $k_1$ reported here is somewhat larger than the ±18% reported by Pirraglia et al. [27] in order to encompass the more recent recommendation of Baulch et al. [6]. Nonetheless, a 40% increase in $k_1$ results in a modest 8% increase in the value of $k_{2,0}$ obtained by fitting the $H_2$ profiles. Uncertainties in $k_3$, $k_{2,\infty}$, and $\Delta H^\circ_{f,HO_2}$ did not significantly influence our determination of $k_{2,0}$.

## Discussion

Figure 4 presents our experimental data for M = $N_2$ in Arrhenius form along with data and recommendations for $k_{2,0}^{N_2}$ from previous studies and reviews. The data of Bromly et al. [12], Davidson et al. [22], and Getzinger and Blair [24] have been used in conjunction with $k_{2,\infty}$ and $F_c^{N_2}$ to determine values of $k_{2,0}^{N_2}$ consistent with their reported values for $k_{2,eff}$. The remaining data were obtained at conditions where reaction 2 is at or near its low-pressure limit and therefore represent measurements of $k_{2,0}^{N_2}$. We have not included data obtained by modeling ignition delays of shock-heated $H_2$–air mixtures because these studies are very sensitive to impurities. All data included in Fig. 4 were derived using profile measurements of stable and intermediate species such as H and OH radicals.

Although in agreement with respect to their combined uncertainties, our experimental data are approximately 40% lower than the recent recommendation of Baulch et al. [6]. Similar disparity is found

TABLE 1
Experimental data

| P [atm] | ave T [K] | M | $\phi$ | $x_{NO,i}$ [ppm] | $k_{2,0}/10^{15}$ [cm$^6$ mole$^{-2}$ s$^{-1}$] | | | |
|---|---|---|---|---|---|---|---|---|
| | | | | | $H_2$ Profile | NO Profile | $NO_2$ Profile | Steady State[a] |
| 10 | 830 | $N_2$ | 0.25 | 101 | 3.73 | 3.69 | 3.54 | 3.55 |
| 10 | 834 | $N_2$ | 0.25 | 107 | 3.77 | 3.84 | 3.99 | 4.23 |
| 12.5 | 838 | $N_2$ | 0.25 | 107 | 4.03 | 3.96 | 3.99 | 4.03 |
| 10 | 855 | $N_2$ | 0.5 | 41 | 3.68 | 3.98 | 3.97 | 3.83 |
| 10 | 862 | $N_2$ | 0.5 | 53 | 3.68 | 3.98 | 3.98 | 4.14 |
| 10 | 882 | $N_2$ | 0.5 | 40 | 3.56 | 3.91 | 3.91 | 3.69 |
| 10 | 819 | Ar | 0.25 | 32 | 2.25 | 2.48 | 2.48 | 2.40 |
| 14 | 819 | Ar | 0.25 | 42 | 2.36 | 2.37 | 2.36 | 2.31 |
| 10 | 823 | Ar | 0.25 | 35 | 2.33 | 2.50 | 2.50 | 2.51 |
| 12 | 826 | Ar | 0.25 | 39 | 2.29 | 2.40 | 2.40 | 2.41 |

[a]Steady-state results represent values of $k_{2,eff} = k_4\,[NO_2]/[O_2]$ averaged over 20–80% extent of reaction.

TABLE 2
Uncertainty analysis

| Parameter | Estimated Uncertainty | Effect on $k_{2,0}$ | |
|---|---|---|---|
| | | M = $N_2$ | M = Ar |
| $k_4$ | ±21% | ±17% | +21%/−17% |
| $F_c$ | ±0.15 | +21%/−9% | +25%/−10% |
| $k_1$ | +40%/−18% | +8%/−6% | +6%/−4% |
| $k_3$ | ±20% | ±5% | ±3% |
| $k_{2,\infty}$ | ±25% | ±2% | ±2% |
| profile fitting | ±10% | ±10% | ±10% |
| Total uncertainty = $\Sigma\,[(\Delta k_{2,0}/k_{2,0})^2]^{1/2}$ | | +30%/−23% | +35%/−23% |

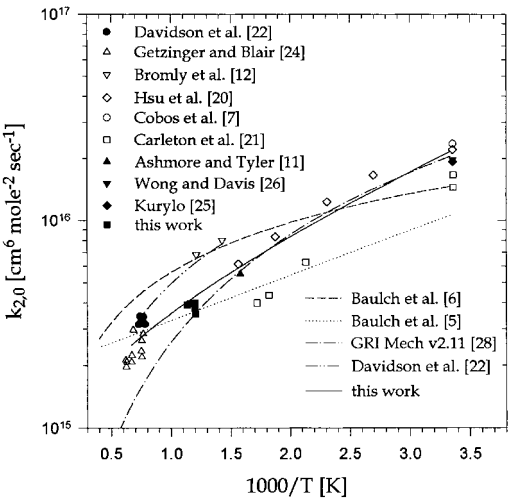


FIG. 4. Arrhenius plot of rate constant data for the reaction H + $O_2$ + $N_2$ → $HO_2$ + $N_2$.

with the recommendation of Davidson et al. [22], who utilized the data of Bromly et al. [12] to extend their temperature range to 700–1375 K. The agreement between our data and the recommendations given in GRI-Mech v2.11 [28] and the earlier review of Baulch et al. [5] is excellent. As shown in Fig. 4, however, the temperature dependencies of these recommendations are quite different and lead to large disparities at the extremes of their temperature ranges. The early Baulch et al. [5] recommendation is in good agreement with the high-temperature data as well as the low-temperature data of Carleton et al. [21], but is much lower than the data of Hsu et al. [20] and nearly a factor of 2 lower than the room-temperature data. While the recommendation of $k_{2,0}^{N_2}$ within GRI-Mech v2.11 generally agrees better with the data at low and intermediate temperatures, it is significantly lower than the high-temperature data.

The disparity between our experimental results and those of Bromly et al. [12] are unexpected and cannot be explained by the differences in the reaction mechanisms used to derive the rate coefficient data for $k_{2,0}$. Although in very good agreement with the recent recommendation of Baulch et al. [6], the data of Bromly et al. are substantially higher than other data obtained at temperatures near the upper (this study) and lower [11,20] limits of their experimental temperature range.

In making our recommendation, we prefer the data of Hsu et al. [20] to that of Carleton et al. [21] for the following reasons. The collection of data from the various studies, as well as those from the individual studies of Hsu et al. and Carleton et al., indicates that reaction 2 has a negative temperature dependency. However, the value of $k_{2,0}^{N_2}$ reported by Carleton et al. at 580 K is nearly equal to our data obtained at temperatures near 850 K and only 25% larger than the high-temperature data reported by Davidson et al. [22]. Furthermore, the room-temperature data of Carleton et al. are somewhat lower than those reported in several other studies [8,20,25,26]. Although we cannot explain the discrepancy between the work of Hsu et al. and Carleton et al., our recommendation of $k_{2,0}^{N_2} = 3.5 \times 10^{16}\, T^{-0.41} \exp(+1116/RT)$ cm$^6$ mole$^{-2}$ s$^{-1}$ incorporates the entire data set shown in Fig. 4 with the exception of the data of Carleton et al. and Bromly et al. [12]. This recommendation is based upon a least-squares analysis in which each data point is weighted equally.

This new rate expression improves the ability of our mechanism [19] to predict the NO-perturbed $H_2/O_2$ reaction over a much broader range of conditions than those used to determine $k_{2,0}^{N_2}$. Indeed, the poor predictive ability of our baseline mechanism using recently published evaluations of $k_{2,0}^{N_2}$ stimulated the present work. Examples of the predictive ability of the modified mechanism are shown in Fig. 5. The agreement at atmospheric pressure is particularly notable because the consumption of $H_2$ is most sensitive to reactions 1 and 2 while being relatively insensitive to reaction 4. We note that the large timeshifts and discrepancy between model

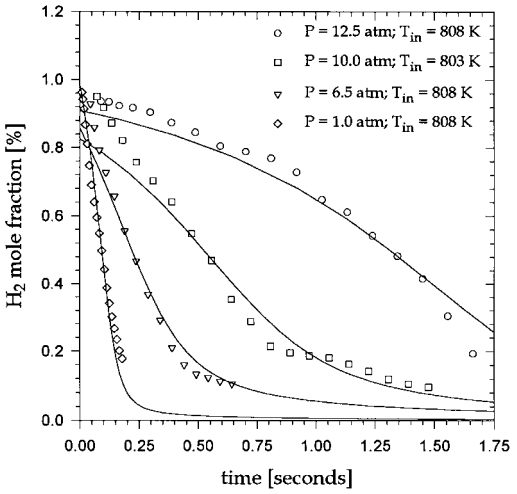


FIG. 5. $H_2$ profiles of 1% $H_2$/2% $O_2$/107 ppm NO/$N_2$ mixtures at pressures ranging from 1 to 12.5 atm. Symbols represent data points; lines represent model predictions generated using $k_{2,0}^{N_2} = 3.5 \times 10^{16}\, T^{-0.41} \exp(+1116/RT)$ $cm^6\ mole^{-2}\ s^{-1}$. For clarity, model predictions have been shifted with respect to the experimental data as follows: 12.5 atm, −0.733 s; 10 atm, −0.588 s; 6.5 atm, −0.142 s; 1 atm, −0.020 s.

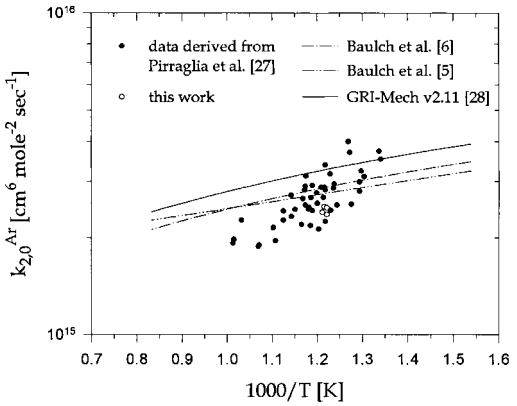


FIG. 6. Arrhenius plot of rate coefficient data for H + $O_2$ + Ar → $HO_2$ + Ar. The combined $(k_1 + k_{2,0}^{Ar}[Ar])$ rate data of Pirraglia et al. [27] have been used with a ratio of $k_1/k_{2,0}^{Ar}$ determined from $H_2/O_2$ explosion limit data to yield the derived data as shown. Relative third-body efficiencies $(\varepsilon_{H_2}:\varepsilon_{O_2}:\varepsilon_{Ar} = 1.0:0.4:0.35)$ as recommended by Ref. [33] were used to estimate $k_1/k_{2,0}^{Ar} = 0.83 \exp(-10{,}310/T)$ mole $cm^{-3}$.

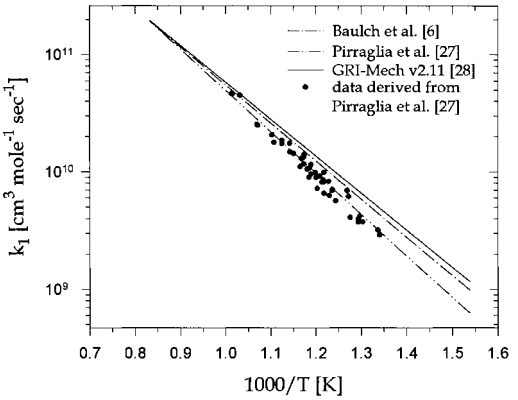


FIG. 7. Arrhenius plot of rate coefficient data for H + $O_2$ → OH + O as derived using $k_1/k_{2,0}^{Ar}$ from explosion limit data and the combined $(k_1 + k_{2,0}^{Ar}[Ar])$ rate data of Pirraglia et al. [27] over the temperature range 746–987 K. The $k_1$ recommendation of Pirraglia et al. is based upon flash photolysis shock-tube data over the temperature range 962–1705 K and the high-temperature (1693–2577 K) data of Frank and Just [35].

predictions and experimental data at 10 and 12.5 atm result from $k_{2,0}^{N_2}$ values (generated using the recommended expression) that are slightly higher than the optimized values obtained in this study. These discrepancies attest to the sensitivity of these experiments to $k_{2,0}^{N_2}$.

Our experimental results for M = Ar are shown in Fig. 6 along with the recommendations for $k_{2,0}^{Ar}$ given in GRI-Mech v2.11 and the reviews of Baulch et al. [5,6]. We also include rate data derived from the experimental results of Pirraglia et al. [27], who measured the combined rates of H + $O_2$ = OH + O and H + $O_2$ + Ar = $HO_2$ + Ar over the temperature range of 746–987 K. By estimating the ratio of $k_1$ to $k_{2,0}$ using $H_2/O_2$ explosion limit data [4,29–32], we used these results to derive rate data for $k_{2,0}^{Ar}$ without assuming a value for $k_1$. As shown in Fig. 6, our experimental data are approximately 15% lower than the recommendations of Baulch et al. and 40% lower than the expression for $k_{2,0}^{Ar}$ within GRI-Mech v2.11 but lie within the scatter of the data derived from Pirraglia et al. Because this larger data set is in good agreement with the recommendations of Baulch et al., our results further support the recommendation for $k_{2,0}^{Ar}$ resulting from these more comprehensive studies.

The analysis of the combined rate data of Pirraglia et al. [27] also yields rate data for $k_1$. These data, given in Fig. 7, show better agreement with the recommendation of Pirraglia et al. [27] than those given in GRI-Mech v2.11 and the recent review of Baulch et al. [6]. The recommendations of Pirraglia et al. and Baulch et al. are based in part on the flash photolysis shock-tube data obtained by Pirraglia et al.

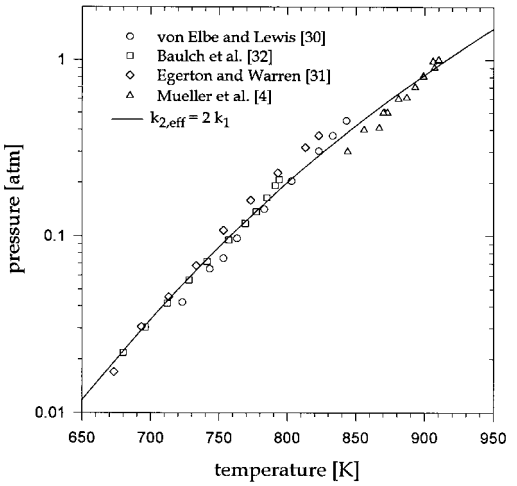


FIG. 8. $H_2/O_2$ explosion limit data along the second limit where $k_{2,\text{eff}} = 2\ k_1$ if $HO_2$ formation is terminating with respect to the radical pool. Relative third-body efficiencies ($\varepsilon_{H_2}$:$\varepsilon_{N_2}$:$\varepsilon_{O_2}$ = 1.0:0.43:0.40) are taken from von Elbe and Lewis [30] and are incorporated into pressure as follows: $p = \text{RT[M]}\ \Sigma_i\ x_i \varepsilon_i$.

[27] over the temperature range 962–1705 K. However, different high-temperature data were used in the two evaluations [34], and the slightly different temperatures dependencies that result produce large differences in $k_1$ at temperatures below 900 K. Due to the importance of the ratio of $k_1$ with respect to $k_2$ at intermediate temperatures, kinetic modeling of the unperturbed $H_2/O_2$ reaction and explosion limit behavior are very sensitive to this discrepancy. As shown in Fig. 8, very good agreement between explosion limit data and model predictions is obtained when the recommendation of Pirraglia et al. is used with our expression for $k_{2,0}^{N_2}$. Together, the two rate constant expressions provide an accurate representation of $k_1/k_{2,0}^{N_2}$ over the temperature range 700–900 K. Recent studies [36] of the ignition of $CH_4/H_2$/air mixtures have recommended increasing the value of $k_{2,0}^{N_2}$ used within GRI-Mech v2.11 in order to satisfy the $H_2/O_2$ ignition limit criterion of $k_{2,\text{eff}} = 2k_1$. We note that this criteria can also be satisfied by using the $k_1$ rate expression of Pirraglia et al. in the intermediate temperature range important for $H_2/O_2$ ignition behavior.

## Summary

New experimental data on the NO-perturbed $H_2/O_2$ reaction have been obtained at pressures and temperatures ranging from 10 to 14 atm and 800 to 900 K, respectively. Kinetic modeling of the $H_2$ and $NO_x$ profiles provided a means to determine rate coefficient data for $k_{2,0}^{N_2}$ and $k_{2,0}^{Ar}$ that are insensitive to $k_1$. Based upon the results of this study as well as previously reported data, we recommend a new expression for $k_{2,0}^{N_2}$:

$$k_{2,0}^{N_2} = 3.5 \times 10^{16}\ T^{-0.41}\ \exp(+1116/\text{RT})$$

$$\text{cm}^6\ \text{mole}^{-2}\ \text{s}^{-1}$$

over the temperature range 300–1600 K. Our experimental data for $k_{2,0}^{Ar}$ are consistent with the shock-tube data of Pirraglia et al. [27] obtained at comparable temperatures and are in good agreement with the recent recommendation of Baulch et al. [6].

*Acknowledgments*

This work was supported by the U.S. Department of Energy, Chemical Sciences Division, Office of Basic Energy Sciences under Contract Number DE-FG02-86ER-13503. The authors also thank Mr. Paul Michniewicz for his assistance in obtaining the experimental data.

## REFERENCES

1. WMO Global Ozone Research and Monitoring Project report number 27, Scientific Assessment of Ozone Depletion: 1994, World Meteorological Organization, Geneva, Switzerland, 1995.
2. Lewis, B. and von Elbe, G., *Combustion, Flames, and Explosions of Gases*, 3rd ed., Academic, Orlando, FL, 1987.
3. Fotache, C. G., Kreutz, T. G., Zhu, D. L., and Law, C. K., *Combust. Flame* 108:442–470 (1997).
4. Mueller, M. A., Yetter, R. A., and Dryer, F. L., "Explosion Limit Behavior of Dilute Hydrogen-Oxygen Mixtures from 0.3 to 3.0 atm and 850–950 K," Eastern States Sectional Meeting of the Combustion Institute, Hilton Head, SC, 1996.
5. Baulch, D. L., Drysdale, D. D., Home, D. G., and Lloyd, A. C., *Evaluated Kinetic Data for High Temperature Reactions*, vol. 1, Butterworth, London, 1972.
6. Baulch, D. L., Cobos, C. J., Cox, R. A., Frank, P., Hayman, G., Just, Th., Kerr, J. A., Murrells, T., Pilling, M. J., Troe, J., Walker, R. W., and Warnatz, J., *J. Phys. Chem. Ref. Data* 23:847–1033 (1994).
7. Cobos, C. J., Hippler, H., and Troe, J., *J. Phys. Chem.* 89:342–349 (1985).
8. Gilbert, R. G., Luther, K., and Troe, J., *Ber. Bunsen-Ges. Phys. Chem.* 87:169–177 (1983).
9. Hippler, H., Troe, J., and Willner, J., *J. Chem. Phys.* 93:1755–1760 (1990).
10. Hippler, H., Neunaber, H., and Troe, J., *J. Chem. Phys.* 103:3510–3516 (1995).
11. Ashmore, P. G. and Tyler, B. J., *Trans. Farad. Soc.* 58:1108–1116 (1962).
12. Bromly, J. H., Barnes, F. J., Nelson, P. F., and Haynes, B. S., *Int. J. Chem. Kinet.* 27:1165–1178 (1995).

13. Ko, T. and Fontijn, A., *J. Phys. Chem.* 95:3984–3987 (1991).
14. Michael, J. V., personal communication, 1997.
15. Held, T. J., Ph.D. thesis, Department of Mechanical and Aerospace Engineering, Princeton University, Princeton, NJ, 1993.
16. Allen, M. T., Yetter, R. A., and Dryer, F. L., *Int. J. Chem. Kinet.* 27:883–909 (1995).
17. Lutz, A. E., Kee, R. J., and Miller, J. A., "SENKIN: A Fortran Program for Predicting Homogeneous Gas Phase Kinetics with Sensitivity Analysis," Sandia National Laboratories report SAND87-8248.
18. Yetter, R. A., Dryer, F. L., and Rabitz, H., *Combust. Sci. Technol.* 79:129–140 (1991).
19. Allen, M. T., Yetter, R. A., and Dryer, F. L., *Combust. Flame* 109:449–470 (1997).
20. Hsu, K.-J., Anderson, S. M., Durant, J. L., and Kaufman, F., *J. Phys. Chem.* 93:1018–1021 (1989).
21. Carleton, K. L., Kessler, W. J., and Marinelli, W. J., *J. Phys. Chem.* 97:6412–6417 (1993).
22. Davidson, D. F., Peterson, E. L., Röhrig, M., Hanson, R. K., and Bowman, C. T., in *Twenty-Sixth Symposium (International) on Combustion*, The Combustion Institute, Pittsburgh, 1996, pp. 481–488.
23. Slack, M. W., *Combust. Flame* 28:241–249 (1977).
24. Getzinger, R. W. and Blair, L. S., *Combust. Flame* 13:271–284 (1969).
25. Kurylo, M. J., *J. Phys. Chem.* 76:3518–3526 (1972).
26. Wong, W. and Davis, D. D., *Int. J. Chem. Kinet.* 6:401–416 (1974).
27. Pirraglia, A. N., Michael, J. V., Sutherland, J. W., and Klemm, R. B., *J. Phys. Chem.* 93:282–291 (1989).
28. Bowmann, C. T., Hansen, R. K., Davidson, D. F., Gardiner, W. C., Lissianski, V., Smith, G. P., Golden, D. M., Franklach, M., and Goldenberg, M., http://www.me.berkeley.edu/gri_mech.
29. Grant, G. H. and Hinshelwood, C. N., *Proc. R. Soc. A* 141:29–40 (1933).
30. von Elbe, G. and Lewis, B., *J. Chem. Phys.* 10:366–393 (1942).
31. Egerton, A. and Warren, D. R., *Proc. R. Soc. A* 204:465–476 (1950).
32. Baulch, D. L., Griffiths, J. F., Pappin, A. J., and Sykes, A. F., *Combust. Flame* 73:163–185 (1988).
33. Warnatz, J., in *Combustion Chemistry* (W. C. Gardiner, ed.), Springer-Verlag, New York, 1985.
34. Michael, J. V., *Prog. Energy Combust. Sci.* 18:327–347 (1992).
35. Frank, P. and Just, Th., *Ber. Bunsen-Ges. Phys. Chem.* 89:181–187 (1985).
36. Fotache, C. G., Ph.D. thesis, Department of Mechanical and Aerospace Engineering, Princeton University, Princeton, NJ, 1997.